Conference on Modelling Fluid Flow (CMFF'06)
The 13th International Conference on Fluid Flow Technologies
Budapest, Hungary, September 6-9, 2006

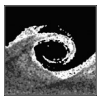

DEVELOPMENT OF A SIMULATION METHOD TO PREDICT UV DISINFECTION REACTOR PERFORMANCE AND COMPARISON TO BIODOSIMETRIC MEASUREMENTS

Christoph REICHL[1], Christoph BUCHNER[2], Georg HIRSCHMANN[3], Regina SOMMER[4], Alexander CABAJ[5]

[1] Corresponding Author. arsenal research – Austrian Research Centers. Giefinggasse 2, 1210 Vienna, Austria. Tel.: +43 50550 6605, Fax: +43 50550 6439, E-mail: Christoph.Reichl@arsenal.ac.at
[2] Technical University of Vienna, arsenal research. E-mail: christoph_buchner@gmx.at
[3] arsenal research. E-mail: Georg.Hirschmann@arsenal.ac.at
[4] Division of Hygiene and Medical Microbiology, Medical University of Vienna. E-mail: regina.sommer@meduniwien.ac.at
[5] Institute of Medical Physics and Biostatistics, University of Veterinary Medicine Vienna. E-mail: alexander.cabaj@vu-wien.ac.at

ABSTRACT

Nowadays, water disinfection with ultraviolet (UV) radiation becomes increasingly important. This work presents a simulation method to predict the disinfection efficacy of an UV disinfection reactor and compares the results to biodosimetric measurements.

CFD calculations have been performed for a set of operation parameters. A discrete phase model was used to generate particle tracks. The fluence rate field inside the reactor has been simulated using several radiation models. Particle tracks and radiation models have been combined to calculate the reduction equivalent fluence (*REF*), an important quantity in biodosimetry. The obtained simulation results are compared to experimental data to assess the achieved accuracy.

The simulated pressure loss of the reactor agreed very well with the experiments. In contrast to the biodosimetric measurements, only a limited amount of data for the flow field and fluence rate distribution is provided by Austrian standard certification procedures. Considering this, good predictions of the *REF* were obtained by the presented simulation method. Average error values varied between 7 and 25%, depending on the chosen radiation model. The potential use of this method for designing and improving UVD reactors has been demonstrated.

Keywords: biodosimetry, CFD, particle tracking, radiation models, REF, UV disinfection

NOMENCLATURE

E'	$[W/m^2]$	fluence rate
H'	$[J/m^2]$	fluence
REF	$[J/m^2]$	reduction equivalent fluence
T	[-]	optical transmittance for 10mm of medium at λ=253.7nm
d	$[m]$	optical path length
dA	$[m^2]$	infinitesimal area
g	$[m]$	length of a cone generatrix
n	[-]	refractive index
r	$[m]$	radial distance
x	$[m]$	axial distance
λ	$[m]$	wavelength
θ	[-]	angle of incidence

Subscripts

1, 2, 3	air, quartz and water, respectively
W, WO	with and without considering refraction, respectively

1. INTRODUCTION

Disinfection of potable and wastewater using additives like chlorine or ozone has a long tradition [1]. However, these treatments can result in the formation of disinfection by-products which are harmful to humans. Additionally, certain microorganisms are particularly resistant to chemical disinfection. Treatment with UV radiation offers a way out, since it is a purely physical process, producing very few by-products compared to chemical methods, and does not alter taste or chemical composition. For this reason, water treatment with UV radiation becomes increasingly important.

Disinfection facilities exist in various sizes, ranging from conventional single-lamp reactors to up to 8000 lamp wastewater installations. Commonly, quasi-monochromatic as well as polychromatic ultraviolet lamps are employed whose radiation permeates the water flow.

Pathogenic microorganisms, which are present in the fluid, are deactivated by the incident photons and lose their danger of infection for humans.

The efficacy of UV disinfection (UVD) reactors strongly depends on several design and operation parameters, namely fluence rate distribution in the reactor chamber, water mass flow and UV transmittance, as well as geometric and hydrodynamic properties of the reactor. This is why great care has to be exercised when adjusting these parameters to achieve optimal operation.

In a normal design process, the last stage is the certification of the reactor for a certain set of operational parameters. In Austria, this certification uses biodosimetric tests (frequently called "bioassay") according to ÖNORM M 5873-1 [2]. If this certification fails, part of the design process has to be repeated. The certification procedure and necessary construction of a prototype is costly and time-consuming. The increasingly powerful numerical simulation techniques available enable the designer to predict reactor performance under certain operating conditions without incurring the high cost of prototype construction and certification. This also makes it possible to examine many different parameter configurations with respect to their performance. In the traditional design process, different operating points need to be certified to determine the disinfection efficacy.

UV disinfection and the associated processes have been investigated by several researchers. The main areas of research are radiation modelling and measurement [3-8], analysis and simulation of the performance of UV disinfection reactors [9-12], bacterial inactivation and repair processes [13-18] and others [19-22]. The guidance manual of the U.S. Environmental Protection Agency [23] provides extensive information on many aspects of the implementation of UV disinfection systems.

The aim of this work is to combine the different aspects of UVD into an overall simulation of a small UVD reactor. This simulation includes Computational Fluid Dynamics (CFD) simulation of the water flow, particle tracking of microorganisms in the water and radiation modelling of the radiation emitted by the UV lamp. As a result, the calculated disinfection efficacy of the UVD reactor is compared to results from three different certification reports [24].

2. METHODS

2.1 Ultraviolet Disinfection

UV light for disinfection applications is produced in mercury vapour arc lamps. In the reactor examined in this work, a low-pressure (LP) lamp was used. This lamp uses mercury vapour with a pressure of <1.3 kPa. This causes one sharp emission line at $\lambda = 253.7\ nm$.

UVD disinfects water by deactivating the contained microorganisms. This happens when high-energy photons of the so-called germicidal band (with a wavelength between 200 and 300nm) cause a transformation of a microorganism's DNA, inhibiting its ability to replicate [19].

2.2 Biodosimetry

The last step in the UVD reactor design process is to check if the reactor reaches the necessary disinfection efficacy under specified operating parameters. This validation is realized with the biodosimetry or bioassay method:

A surrogate (challenge) microorganism is injected into the water flowing through the UVD system. The reduction (i.e. the fraction of surviving microorganisms) is measured for a set of desired operating parameters (mainly flow rate, water UV transmittivity and lamp power) by cultivating and counting water samples from before and after the reactor. Since the delivered UV fluence (see section 2.6 for a definition) cannot be measured directly, the received fluence has to be related to the surrogate microorganism's reduction in a separate test. This relation, the survival curve, is normally generated with a collimated beam experiment beforehand. This curve is used to determine the reduction equivalent fluence (*REF*) from the reduction values (see section 2.6).

The Austrian standard for UV disinfection with LP UVD reactors, ÖNORM M 5873-1 [2], requires a minimum *REF* of 400 J/m^2 and *Bacillus subtilis* spores as a challenge microorganism. The spores are roughly cylindrical with approximately 1μm in length and 0.5μm in diameter. A detailed description of certification processes can be found in [23].

Recently, the actual fluence distribution of a reactor has been measured using fluorescent microspheres. This technique could improve confidence in the use of mathematical models for UVD and complement biodosimetry testing [3].

2.3 The UVD reactor

The modelled reactor is a single low-pressure lamp, closed-channel, axial flow reactor designed for flow rates ranging from 0.7 to 6m^3/h, with a lamp power rating from 60 to 130W.

As can be seen in Figure 1, the model of the reactor comprised not only the reactor chamber itself, but also an inlet region before the inlet pressure sensor, an elbow connected to the reactor vessel and an outlet pipe. It was important to include these segments into the actual simulation, because they mimicked the situation at validation as closely as possible, and they had a great influence on the velocity distribution of the flow when entering the reactor. The reactor vessel had an inner diameter of 100mm and a length along the main axis of 1048mm. The quartz sleeve protecting the UV

lamp was located along the main axis of the reactor and had an outer diameter of 30*mm*, running along the entire length of the reactor. The inlet and outlet pipes had several different diameters ranging from 37 to 43*mm*, creating several forward and backward facing steps in those regions. Shortly above the reactor vessel inlet, an annular plate with 8 evenly spaced circular holes was welded into the reactor.

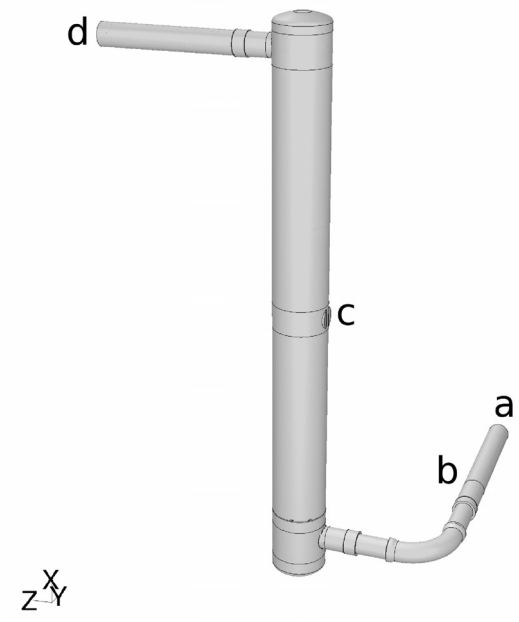

Figure 1. 3D model of the UVD reactor. *a:* water inlet, *b:* pressure sensor, *c:* UV sensor window, *d:* water outlet

2.4 Computational Fluid Dynamics

The mesh of the reactor consisted of approximately 3 million cells, with the smallest cells 1.2*mm* in size. Additionally, a mesh adaptation was made to improve resolution where necessary.

From the validation reports, data for 23 different sets of operational parameters ("cases") were available. For these cases, steady-state calculations have been carried out with the CFD package Fluent, using the realizable-k-ε turbulence model. Additionally, for one case, the elbow has been transformed into a straight pipe to judge the influence of the elbow on the disinfection performance. Thus, the disinfection simulation could be performed for 24 different cases encompassing the whole operational spectrum of the UVD reactor.

It is possible that significant fluctuations occur in the water flow, which influence disinfection results, but cannot be reproduced by steady-state calculations. Unfortunately, at the time being, unsteady calculations were computationally too expensive to perform, especially in light of potential future industry applications of UV disinfection simulation.

2.5 Particles

Particle tracking was performed for simulated *Bacillus subtilis* spores having the density of the surrounding water.

The particle tracking was performed with a ready-made discrete phase model: Particle tracks are calculated by solving the force balance equation for the particle in question. A formulation for non-spherical particles was used in the drag term to account for the cylindrical form of the particles [25].

Particles were injected at every cell location of the inlet face, which resulted in 1666 particles. This number was too small for reliable calculations. Thus, a stochastic tracking approach using a random-walk model was included. In this approach, the interaction of a particle with a succession of discrete stylized fluid phase turbulent eddies is simulated. Each eddy is characterized by a Gaussian distributed random velocity fluctuation and a time scale. The magnitude of the velocity fluctuation is calculated with the turbulent kinetic energy and a random number. Using this model, multiple non-identical particle paths ("tries") can be computed for a single cell on the inlet face. Thus, the number of particles can be increased, only limited by the memory capacity of the calculating workstation. It has been found that 16 tries, resulting in approximately 26600 particle paths, were a good compromise between accuracy and computational demand.

The spores are small enough and in such low concentrations that an interaction with the fluid phase could be ruled out.

2.6 Radiation

The main relevant radiation quantities in UVD are:

• *Fluence rate (E'):* the radiant power passing from all directions through an infinitesimally small sphere of cross-sectional area *dA*, divided by *dA*. Fluence rate and irradiance are similar, but conceptually quite different terms. Since a microorganism can receive UV radiation from any direction (especially with multiple lamps involved), fluence rate is the appropriate term to use in a UV reactor *[8]*.

• *Fluence or UV Dose (H'):* defined as the total radiant energy from all directions passing through an infinitesimally small sphere of cross-sectional area *dA*, divided by *dA*. The fluence is the fluence rate times the irradiation time in seconds *[8]*.

• *Reduction equivalent fluence (REF):* To be able to compare different reactor designs, which may have been evaluated with different challenge microorganisms, the reduction is unsuitable. To obtain a more comparable quantity, the fluence distribution has to be weighted with the survival curve, yielding the *REF*. This quantity can easily be calculated by forming the inverse function of the

survival curve, and inserting the calculated total reduction [2, 16].

2.6.1 Optics

In UVD reactors, UV radiation from the lamp has to travel through a layer of air surrounding the lamp and pass the quartz sleeve encasing the lamp before it reaches the water to be disinfected. This causes the radiation to be attenuated by the reflection and absorption processes as it travels along the optical path. A depiction of these different factors and a typical optical path for the examined UVD reactor is shown in Figure 2. Furthermore, values for the relevant optical parameters used in this work are given in Table 1.

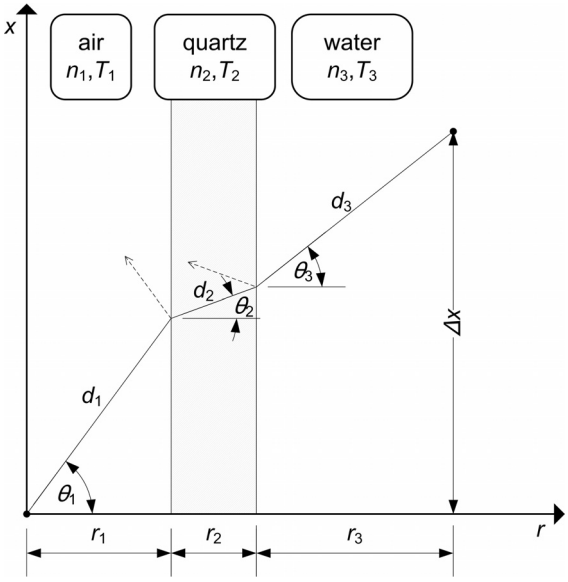

Figure 2. Optical path in the UVD reactor: Light is travelling from the source on the x-axis to the destination coordinate

Table 1. Optical parameters of the examined reactor at $\lambda = 254nm$. Transmittance values are for 10mm of material

	Air	Quartz	Water
Refractive index	n_1 1	n_2 1.506	n_3 1.376
Transmittance	T_1 1	T_2 0.8208	T_3 differs
Layer thickness	r_1 13mm	r_2 2mm	$r_{3,\max}$ 35mm

It has been found [8] that for drinking water applications (with a water transmittance of $T_3 >$ 0.7), the effects of refraction and reflection at media interfaces have to be included to permit an accurate calculation.

2.6.2 Focus effect

Another component of refraction is the focus effect [9]. Considering no refraction, the radiation power emitted from a point source within a finite difference angle $2\Delta\theta_1$ (see Figure 3) and travelling for a distance of $d_1+d_2+d_3$, would cover a circle with a diameter of g_{WO}. When exploiting the cylindrical symmetry of the lamp, this cross-section becomes a frustum or truncated cone of area A_{WO} with an aperture angle of $2\theta_1$, the lamp axis as frustum axis and the generatrix g_{WO}.

Now, when including refraction at the media interfaces, while keeping the optical path length $d_1+d_2+d_3$ constant, this frustum has the area A_W, the aperture angle $2\Delta\theta_3$ and the generatrix g_W.

Liu [9] introduced the so-called focus factor, which describes the extent by which the focus effect concentrates the light, thus changing the fluence rate at any given point. This focus factor is the ratio of the two aforementioned frustum areas A_{WO} and A_W. It has been calculated to:

$$Focus = \frac{(d_1 + d_2 + d_3)^2}{(r_1 + r_2 + r_3)\cos\theta_3 n_1} \cdot \left(\frac{r_1}{n_1 \cos^3\theta_1} + \frac{r_2}{n_2 \cos^3\theta_2} + \frac{r_3}{n_3 \cos^3\theta_3} \right) \quad (1)$$

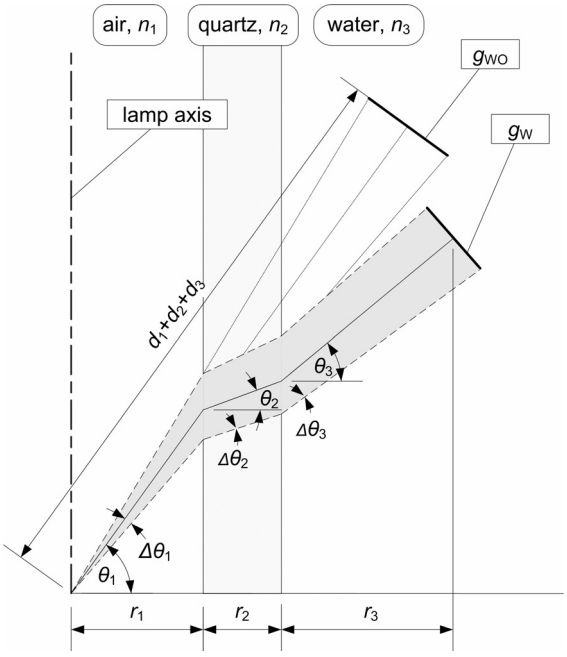

Figure 3. The focus effect: The optical path with and without refraction and the resulting generatrices g_W and g_{WO} for the focus effect calculation are shown

2.6.3 Radiation modelling

For all radiation models treated in this section, the fluence rate has been calculated with self-developed routines for a cylindrical grid which filled the reactor chamber.

A refinement study has been performed to obtain the necessary grid resolution. The fluence rate along several straight paths was evaluated for increasingly coarse grids. The deviation of said values from the values for the smallest computationally possible cell size was computed. The size of the grid cells at the outer quartz sleeve surface was determined by deciding that neither the maximum deviation nor the mean + 3 standard deviations for any given path should exceed 1%. It was found that a cell size of $2mm$ was sufficient for this criterion.

To successfully calculate the fluence rate, the calculation of the refraction angles θ is necessary. The relevant relation, Eq. (2), can be found by using Snell's law and trigonometry. To ease calculation, all angles have been related to θ_1.

$$r_1 \tan\theta_1 + n_1 \sin\theta_1 \frac{r_2}{\sqrt{n_2^2 - n_1^2 \sin^2\theta_1}} + \\ + n_1 \sin\theta_1 \frac{r_3}{\sqrt{n_3^2 - n_1^2 \sin^2\theta_1}} = \Delta x \qquad (2)$$

Unfortunately, this equation can only be solved numerically. This was accomplished with Brent's method, a root finding algorithm described in [26]. After finding θ_1, all other optical quantities can easily be calculated.

Several radiation models have been implemented:

The Multiple Point Source Summation with focus effect (**MPSS-F**) represents the UV lamp as a number of point sources. The fluence rate at a certain point in the reactor is calculated by summing up the fluence rate values of all point sources. The focus effect has been included in this model.

In the Multiple Segment Source Summation (**MSSS**) model, the point sources are replaced by cylindrical segment sources, resulting in an additional cos θ_1 term. This model has also been included with the focus effect (**MSSS-F**). MSSS-F models the physical processes most closely of all presented models.

The Line Source Integration (LSI) model is the continuous or integral version of the MPSS model. These models are mathematically identical as the number of point sources approaches ∞ [9]. However, a computationally fast closed-form solution only exists in absence of absorption, reflection and refraction. To correct for this shortcoming, Liu [9] developed the attenuation factor approach, where the LSI model is multiplied with a correcting attenuation factor. In this work, an attenuation factor which used the MSSS-F model was used (**LSI-F**).

Bolton and Liu developed a modified form of the LSI model to correct inaccuracies when approaching the quartz sleeve [9]. This model, called **RADLSI**, was implemented with a MPSS attenuation factor.

A more extensive description of the different models can be found in [9].

2.6.4 Refinement

Again, a refinement study has been done to find the number of necessary sources for the different radiation models.

For the MPSS and MSSS models, the fluence rate at 4 points in the reactor volume was calculated using a MSSS-F model with an increasing number of sources ranging from 10 to 10000. Afterwards, it was decided that to be sufficiently accurate, the calculated fluence rate at any point should not deviate by more than 1% from the value for 10000 sources. This was deemed to sufficiently represent the fluence rate in the limit of an infinite number of sources. It was found that 2000 sources were sufficient to fulfil this criterion. Thus, 2000 sources were used for the MPSS/MSSS models.

An important advantage of LSI models over MPSS/MSSS is the greatly reduced computational cost. Thus, choosing 2000 sources, while being very accurate, is impracticable because it would neutralize this advantage. When plotting fluence rate values of axial paths, it turns out that an insufficient number of sources leads to unnatural oscillations in the fluence rate distribution. Since these oscillations are worst at small distances to the lamp, a path adjacent to the quartz sleeve was evaluated. It was found that 100 sources were enough to eliminate the unphysical oscillations when using LSI models.

2.6.5 UV reference sensor

An important part of the radiation calculation is the determination of the irradiance of the UV reference sensor in the reactor vessel: This value was the only available radiation measurement with which to check the radiation model. Unfortunately, the conversion efficiency from electrical power to light at $253.7nm$ is not measured during certification processes, and only the electrical power rating was given in [24]. Furthermore, some validation cases use reduced lamp power to simulate an aged lamp near the end of its designated lifetime.

For these reasons, a sensor simulation was developed, including the known sensor assembly geometry and parameters into a MSSS-F model. With this sensor model, the radiation models were calibrated. The MSSS-F model was deemed most appropriate for this task since it matches the

occurring physical processes best of all treated radiation models. The UV conversion efficiency was adjusted such that the simulated sensor reading equalled the experimental reading from the validation reports.

2.6.6 Disinfection calculation

When particle tracks and fluence distribution are known, a fluence value is calculated for each particle. This fluence value is combined with the survival curve to determine the reactor's reduction. From the reduction, the *REF* is easily calculated.

3. RESULTS

3.1 CFD

To compare the CFD results against the experiments, pressure loss data were available from the validation reports. A quadratic fit (R^2=0.9981) has been calculated, and the CFD pressure loss information has been compared to these two data sets. The mean of the absolute values of the error (in %) has been calculated. Compared to the experiment and fit, mean values of 5.4 and 3.2%, respectively, have been obtained.

Replacing the elbow with a straight pipe reduced the pressure loss by 6.6%. It has been found that the inlet pipe is responsible for about 50% and the reactor chamber for about 40% of the pressure loss.

3.2 Radiation models

The fluence rate distribution has been evaluated along several axial and radial paths in the reactor. Reactor validation according to ÖNORM M 5873-1 [2] does not demand a laborious measurement of the radiation distribution in the reactor. Thus, only the reference sensor data were available. This data already being needed for the UV efficiency calibration, the different radiation models could only be compared among themselves.

It has been found that there is an excellent agreement between the MSSS-F and LSI-F models. This is consistent with findings in [9].

Calculating a fluence rate field for the reactor with the MSSS-F model takes approximately 17 times as long as with a LSI-F model. Therefore, using the LSI-F model seems to be highly tempting. However, one should keep in mind that the fluence rate calculation takes a rather small part of the computation time compared to particle track generation and particle fluence calculation, especially for a high number of particle tracks.

When comparing the MSSS, MSSS-F and MPSS-F results, it can be concluded that the influence of the focus effect (i.e. the difference between MSSS and MSSS-F) is far smaller than the influence of the segment source representation (i.e. the difference between MPSS-F and MSSS-F). Thus, it was concluded that implementing segment sources is definitely necessary. Fortunately, this does not measurably increase computation time, and thus has no drawbacks.

3.3 Disinfection

Disinfection simulations have been performed for 24 cases. Figure 4 shows the *REF* values obtained with the UVD simulation. Black crosses are the experimental results with error bars from [24]. The different results have been connected with lines only to guide the eye and facilitate analysis.

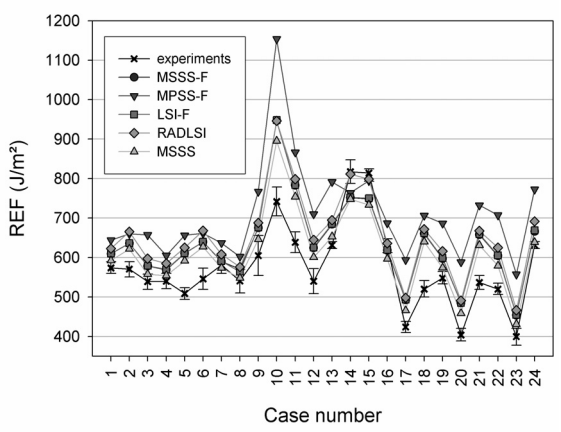

Figure 4. Disinfection simulation results: *REF*. The simulated *REF* values for the different cases and experimental results with error bars are shown. Connecting lines have been added to ease analysis

As expected from the fluence rate distributions, the MPSS-F model generally produces the highest *REF* values. All other plots typically are very close together. Also, MSSS-F and LSI-F produce nearly identical results - the MSSS-F plot is not visible because it lies behind the LSI-F plot. This further confirms that the LSI-F model is a good approximation of the MSSS-F model.

Figure 5 shows a plot of the relative errors of the different radiation models. An analysis of the error value distribution has been done. Mean value and standard deviation of the errors have been calculated for all radiation models and cases, excluding the case with the straightened elbow (case 24) because it has a different geometry. The results can be found in Table 2.

Table 2. Error statistics. Mean value and standard deviation of *REF* simulation errors (in %) are given for different radiation models

	MSSS-F	MPSS-F	LSI-F	RADLSI	MSSS
mean	11.58	24.65	11.71	14.64	7.54
σ	9.90	15.37	9.97	9.06	8.93

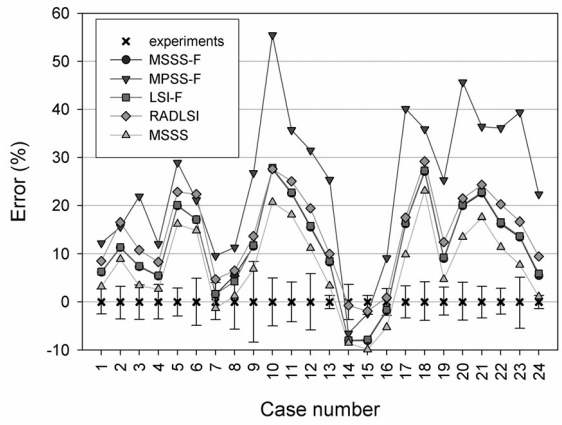

Figure 5. Disinfection simulation results: relative error. The relative error is plotted for the different cases. Connecting lines have been added to ease analysis

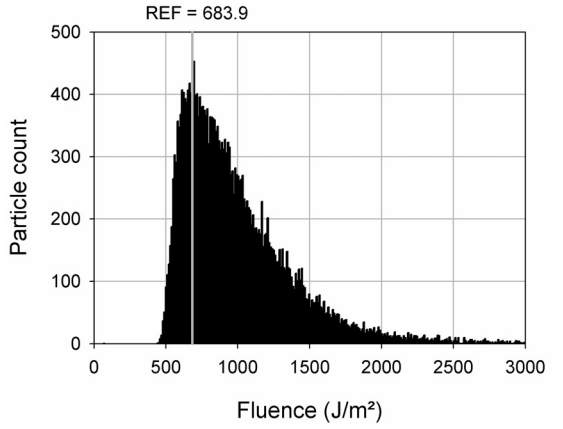

Figure 6. Calculated fluence histogram for case 13 using the MSSS-F model. The resultant *REF* of the fluence distribution is indicated

The MSSS model produces the smallest mean error, and also the smallest standard deviation. MSSS-F and LSI-F rank next, producing virtually identical results. RADLSI comes next, and MPSS-F produces the least accurate results. However, one has to keep in mind that the UV efficiency was used to calibrate the radiation models such that the experimental reference sensor reading is matched by the MSSS-F model. A different UV efficiency value would shift all *REF* results up or down, thus changing the error values and the ranking of the different radiation models.

The consistently positive mean values show that all radiation models generally over-predict the *REF* values. This over-prediction may be corrected by shifting the resultant *REF* values by a certain value. However, the amount of this shift may be influenced by e.g. geometry, and thus cannot be assumed to be generally valid.

3.3.1 Straight inlet pipe

The *REF* values for the different radiation models for case 24 show an average drop in *REF* of 2% compared to the same case with an elbow (case 13). This does not seem to be significant as such a fluctuation is very small.

3.3.2 Fluence histograms

Using the data from the UVD simulation, fluence histograms can easily be calculated. Figure 6 displays a typical histogram, showing the fluence distribution for case 13 using the MSSS-F model. The resultant *REF* of the fluence distribution is additionally shown. The x-axis scale has been limited to 3000 J/m^2 to improve display of the relevant portion of the fluence histogram. Actual fluence values reach up to 5200 J/m^2, but the particle counts are negligibly small above the chosen limit.

4. CONCLUSIONS

A simulation method to predict UV reactor disinfection performance has been presented. Calculations have been performed for several radiation models and have been compared to biodosimetric measurements. Considering the limited amount of available experimental data for the flow field and fluence rate distribution, good predictions of the *REF* were obtained. The potential use of this method for designing and improving UVD reactors has been demonstrated.

Future work will encompass unsteady CFD calculations, which will yield unsteady particle tracks. Furthermore, different reactor geometries can be examined. Ray-tracing can additionally be employed to include reflection at the reactor walls.

REFERENCES

[1] Gelzhäuser, P., Bewig, F., Holm, K., Kryschi, R., Reich, G., and Steuer, W., 1985, *Desinfektion von Trinkwasser durch UVBestrahlung*, vol. 182 of *Kontakt & Studium*, Technische Akademie Esslingen and expert verlag.

[2] Österreichisches Normungsinstitut, 1021 Wien, 2001, *ÖNORM M 5873-1: Anlagen zur Desinfektion von Wasser mittels Ultraviolett-Strahlen - Anforderungen und Prüfung - Teil 1: Anlagen mit Quecksilberdampf-Niederdruckstrahlern*.

[3] Bohrerova, Z., Bohrer, G., Mohanraj, S. M., Ducoste, J., and Linden, K. G., 2005, "Experimental Measurements of Fluence Distribution in a UV Reactor Using Fluorescent Microspheres", *Environ. Sci. & Technol.*, vol. 39, pp. 8925-8930, accepted August 29, 2005.

[4] Ducoste, J. J., Liu, D., and Linden, K., 2005, "Alternative Approaches to Modeling Fluence Distribution and Microbial Inactivation in

Ultraviolet Reactors: Lagrangian versus Eulerian", *Journal of Environmental Engineering*, vol. 131, pp. 1393-1403.

[5] Ducoste, J. and Linden, K., 2005, "Determination of ultraviolet sensor location for sensor set-point monitoring using computational fluid dynamics", *J. Environ. Eng. Sci.*, vol. 4, pp. 33-43.

[6] Jin, S., Linden, K. G., Ducoste, J., and Liu, D., 2005, "Impact of lamp shadowing and reflection on the fluence rate distribution in a multiple low-pressure UV lamp array", *Water Research*, vol. 39, pp. 2711-2721.

[7] Bolton, J. R., Wright, H., and Rokjer, D., 2005, "Using a mathematical fluence rate model to estimate the sensor readings in a multi-lamp ultraviolet reactor", *J. Environ. Eng. Sci.*, vol. 4, pp. 27-31.

[8] Bolton, J. R., 2000, "Calculation of ultraviolet fluence rate distribution in an annular reactor: Significance of refraction and reflection", *Wat. Res.*, vol. 34, pp. 3315-3324.

[9] Liu, D., 2004, "Numerical Simulation of UV disinfection reactors: Impact of fluence rate distribution and turbulence modeling", Ph.D. thesis, North Carolina State University.

[10] Chiu, K., Lyn, D., Savoye, P., and III, E. B., 1999, "Integrated UV Disinfection Model Based in Particle Tracking", *Journal of Environmental Engineering*, vol. 125, pp. 7-16.

[11] Downey, D., Giles, D., and Delwiche, M., 1998, "Finite element analysis of particle and liquid flow through an ultraviolet reactor", *Computers and Electronics in Agriculture*, vol. 21, pp. 81-105.

[12] Buffle, M.-O., Chiu, K.-P., and Taghipour, F., 2000, "UV reactor conceptualization and performance optimization with computational modeling", *Proceedings WEF Specialty Conference on Disinfection*, New Orleans, LA.

[13] Kowalski, W., Bahnfleth, W., Witham, D., Severin, B., and Whittam, T., 2000, "Mathematical Modeling of Ultraviolet Germicidal Irradiation for Air Disinfection", *Quantitative Microbiology*, vol. 2, pp. 249-270.

[14] Zimmer, J. and Slawson, R., 2002, "Potential Repair of *Escherichia coli* DNA following Exposure to UV Radiation from Both Medium- and Low-Pressure UV Sources Used in Drinking Water Treatment", *Applied and Environmental Microbiology*, vol. 68, pp. 3293-3299.

[15] Cabaj, A., Sommer, R., Pribil, W., and Haider, T., 2002, "The spectral UV sensitivity of microorganisms used in biodosimetry", *Water Science and Technology: Water Supply*, vol. 2, pp. 175-181.

[16] Cabaj, A. and Sommer, R., 1999, "Measurement of UV-Radiation with Microorganisms (Biodosimetry)", R. Matthes and D. Sliney (editors), *Measurements of Optical Radiation Hazards, A Reference Book*, ICNIRP, CIE.

[17] Cabaj, A., Sommer, R., and Schoenen, D., 1996, "Biodosimetry: Model calculations for UV water disinfection devices with regard to dose distributions", *Water Research*, vol. 30, pp. 1003-1009.

[18] Mamane-Gravetz, H., Linden, K. G., Cabaj, A., and Sommer, R., 2005, "Spectral Sensitivity of *Bacillus subtilis* Spores and *MS2 Coliphage* for Validation Testing of Ultraviolet Reactors for Water Disinfection", *Environmental Science and Technology*, vol. 39, pp. 7845-7852.

[19] Das, T. K., 2001, "Ultraviolet disinfection application to a wastewater treatment plant", *Clean Products and Processes*, vol. 3, pp. 69-80.

[20] Das, T. K., 2002, "Evaluating the life cycle environmental performance of chlorine disinfection and ultraviolet technologies", *Clean Technologies and Environmental Policy*, vol. 4, pp. 32-43.

[21] U.S. Environmental Protection Agency, 1999, "Ultraviolet Disinfection", *Wastewater Technology Fact Sheet*.

[22] Jeyanayagam, S. and Bryck, J., 2002, "Practical Considerations in the Use of UV light for Drinking Water Disinfection", presented at the International Conference on Environmental Engineering in Niagara Falls, Ontario, Canada.

[23] U.S. Environmental Protection Agency, 2003, *Ultraviolet Disinfection Guidance Manual, Draft,* Washington, DC.

[24] Hirschmann, G., Cabaj, A., Sommer, R., Mann, M., Pascoli, G., Windischbauer, G., and Rotter, M., 2004 and 2005, "Biodosimetrische und strahlungsmesstechnische Untersuchung einer UV-Desinfektionsanlage für Trinkwasser mit Niederdruck Quecksilberdampfstrahler, ", 3 te*chnological reports*, ÖFPZ Arsenal Ges.m.b.H., Veterinärmedizinische Universität Wien, Medizinische Universität Wien.

[25] Fluent Inc., Lebanon, NH, USA, 2005, *FLUENT 6.2 User's Guide*.

[26] Press, W. H., Teukolsky, S. A., Vetterling, W. T., and Flannery, B. P., 1992, *Numerical Recipes in C, The Art of Scientific Computing*, Press Syndicate of the University of Cambridge, 2nd edition.